

Biomedical Physics & Engineering Express



PAPER

The synthesis of a liver tissue mimicking solution for microwave medical applications







OPEN ACCESS

RECEIVED
22 March 2022

REVISED
1 July 2022

ACCEPTED FOR PUBLICATION
23 August 2022

PUBLISHED
6 October 2022

Iman Farhat , Jonathan Farrugia , Lourdes Farrugia , Julian Bonello , Daphne Pollacco  and Charles Sammut 

Physics Department, University of Malta, Misda, Malta

E-mail: iman.farhat@um.edu.mt

Keywords: tissue mimicking solution, dielectric properties, types of tissue-like phantoms, Bruggemann mixture equation

Original content from this work may be used under the terms of the [Creative Commons Attribution 4.0 licence](https://creativecommons.org/licenses/by/4.0/).

Any further distribution of this work must maintain attribution to the author(s) and the title of the work, journal citation and DOI.



Abstract

This paper presents the synthesis of a mixture solution that is equivalent to ex-vivo liver tissue dielectric characteristics between 500 MHz and 5 GHz. The mimicking solution was synthesized using concentrations of two chemicals, the solute which is referred to as the inclusion phase and the solvent, referred to as the host phase. The inclusion phase consisted of bovine serum albumin (BSA) powder and the host phase consisted of a phosphate-buffered saline (PBS) solution with a concentration of Triton X-100 (TX-100). The dielectric properties of these two phases were substituted into Bruggeman's two-phase mixture equation to estimate the dielectric properties of excised liver. Furthermore, the study exploits Bruggeman's equation to investigate the impact of tissue dehydration levels on the dielectric properties of an excised tissue. The effect of dehydration has been characterised as a function of time based on the loss-on-drying technique (a substance is heated until it is completely dry). Dielectric parameters were measured as a function of frequency using the Slim Form open-ended coaxial probe at a constant room temperature of circa 25 °C. Measured dielectric data were fitted to the Cole-Cole model and good agreement with the mimicking solutions was obtained. These results indicate that these solutions can be used to model the human body phantoms for microwave medical applications.

1. Introduction

The rapid expansion of electromagnetic (EM) applications in biology and medicine has illustrated significant interest in studying the interactions of EM waves with biological tissues, in particular at microwave frequencies. Therefore, the desire for anatomical phantoms that simulate the EM properties of tissues at microwave frequencies has dramatically increased. Accurate simulation of dielectric properties of biological tissues is invaluable to evaluate technological imaging challenges concerning therapeutic device performance and medical procedures in a test environment avoiding necessary risk to animal or human subjects [1]. Hence, it is crucial for advancements in EM phantom development [2]. In this paper, we establish a link between experiment and mathematical modeling of the dielectric properties of tissues. This gives confidence in the developed method to synthesize tissue mimicking solutions for the development of

phantoms operable in the Microwave (MW) regime, as reported in [3].

Over the years, many different tissue-mimicking materials (TMMs) used for phantoms with desired EM dielectric properties were developed to appropriately model liver human tissue for calibration of the EM medical systems [4]. TMMs exist in many forms, classified as liquid tissue phantoms, solid silicone or polymer phantoms, gelatin/agarose phantoms, and animal phantoms [5], as depicted in figure 1.

Several materials have been used to develop an ideal liver phantom based on solid or dry TMMs, which are usually formed from polyacrylamide gel (PAG), oil-in-gelatin, and carbon-based synthetics [9, 10]. The PAG mimic constitutes Acrylamide (C₃H₅NO) polymerized in a liquid solvent, and it is used as a biological equivalent for microwave hyperthermia or scaled-phantom experiments, which are usually prepared to study full-scale man exposure to EM radiation and simulate absorption characteristics

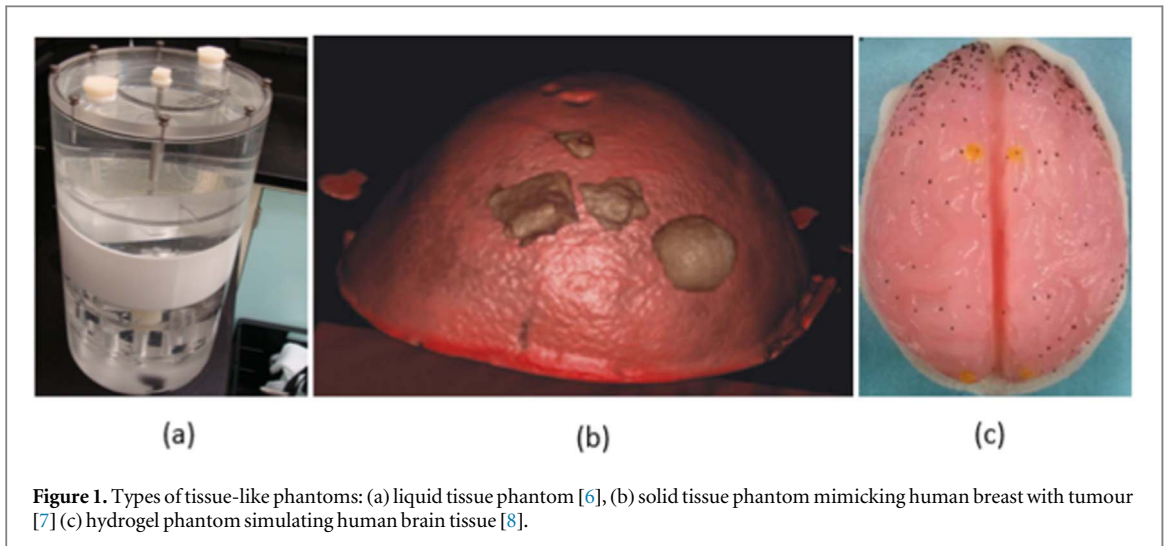


Figure 1. Types of tissue-like phantoms: (a) liquid tissue phantom [6], (b) solid tissue phantom mimicking human breast with tumour [7] (c) hydrogel phantom simulating human brain tissue [8].

[11]. Furthermore, PAG with concentrations of BSA is used for ultrasound and radiofrequency ablation studies [10]. This recipe provides excellent optical transparency and high elasticity. However, when fabricated as phantoms, it suffers from a short lifetime usage lasting for only several hours when exposed to air or several weeks when stored in a tightly-covered container [9]. Solid phantoms can also be fabricated from water, sugar, NaCl, and HEC gelling agents as described in [12]. Liquid tissue equivalent phantoms are preferred for performing power deposition (SAR) studies employing electric field distributions. Appropriate liquid human liver phantoms were established by mixing ethylene glycol iteratively, NaCl, and water to achieve the best match of dielectric properties at the most commonly used microwave heating frequency of 915MHz [12]. However, accurate mimicking of solution phantoms for the liver over a wide range of microwave frequencies from 0.5-5 GHz has not been reported previously. Moreover, previous liquid phantoms are based on specifications related to optical and dynamic properties [13]. This paper focuses on the dielectric properties characterization of liver at frequencies from 0.5-5 GHz and subsequent mimicking solution for a homogenous liver that accurately models the average electrical properties of the liver.

The liquid TMMs are the easiest and most flexible phantoms to fabricate in volume and consistency. Their preparation procedure is rapid and not complicated when compared to other TMMs. The liquid nature of tissue phantoms allows for significant flexibility in sample measurements, and the container material can vary depending on the application. This paper adopts a mixture equations procedure that is employed by Pollacco *et al* (2019) which was used for developing tissue-mimicking solutions for muscle and adipose [3]. The study correlates findings from experimental observations and theoretical results by employing both Bruggeman and Maxwell Garnett mixture equations at different hydration states. The Bruggeman mixture findings were best to reproduce

the experimental dielectric data obtained from measurements. Here, we present a recipe to fabricate a liquid phantom based on the Bruggeman mixture equation to simulate the dielectric properties of liver tissue for different dehydration levels, considering solutions of distilled water with PBS and concentrations of BSA. The goal of this work was to develop a protocol for a novel liver mimicking solution at microwave frequencies that is suitable for MW medical applications. The entire procedure is advantageous as the preparation is simple and rapid—it takes around an hour to prepare. In the next sections, the method, the mixture solution procedure, results, and some concluding remarks and key findings are presented.

2. The theoretical framework

In general, mixing equations are mathematical formulas that model materials' macroscopic dielectric properties based on their constituent components' dielectric properties. The Bruggemann mixing model presented is based on a two-component mixture, the host phase, which represents a homogeneous background, and the inclusion phase, which represents reliable spherical insertions inside the background. The Bruggemann two-component mixture equation is given by equation (1) [3, 14]:

$$\varepsilon_{\text{eff}} = \frac{1}{4}(3v_f\varepsilon_h - 3v_f\varepsilon_i + 2\varepsilon_i - \varepsilon_h) + \sqrt{(3v_f\varepsilon_h - 3v_f\varepsilon_i + 2\varepsilon_i - \varepsilon_h)^2 + 8\varepsilon_i\varepsilon_h} \quad (1)$$

where ε_h is the permittivity of the host environment, ε_i is the permittivity of the inclusion phase, ε_{eff} is the effective permittivity of the material and v_f is the volume fraction of the host medium.

In this study, biological tissues are considered to consist of a mixture of extracellular fluid and extracellular macromolecules (proteins). Therefore, the

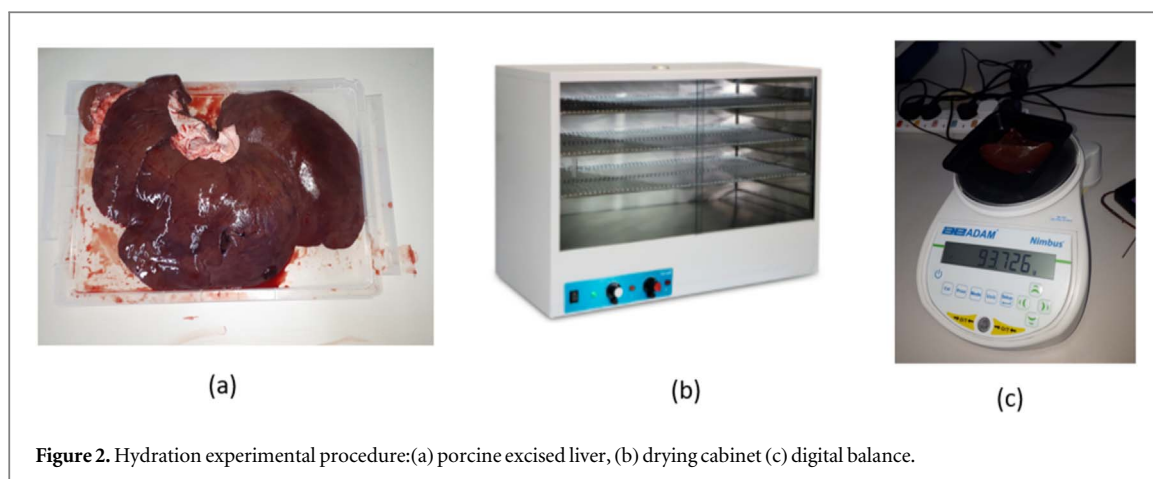


Figure 2. Hydration experimental procedure:(a) porcine excised liver, (b) drying cabinet (c) digital balance.

host medium is represented by the biological fluid within the tissue and the dry biological component. The volume fraction v_f refers to the biological fluid whilst $(1 - v_f)$ is the volume fraction of the inclusion phase made up of the dry biological component. The dielectric properties of the biological tissues were determined using the measurement setup discussed in section 3.2. The method is similar to that published in [3] used to develop an experimental liquid phantom for muscle and adipose. Different stages of dehydration were considered in this study. However, it was challenging to measure the dielectric properties of a dry tissue texture using an open-ended coax technique.

3. Materials and methods

In this section, the chemicals and materials used alongside with the synthesis and dielectric measurement procedures will be discussed.

3.1. Fluid content and dehydration measurements

A measurement campaign to determine the fluid content of different biological tissues was conducted on liver samples extracted from five porcine and ovine animals as explained in [15]. Samples were obtained and preserved in sterile plastic bags after being harvested within an hour of animal death, see figure 2(a). Then, the biological fluid content of the samples was determined using the loss-on-drying method [16], where samples were equally divided into small-scale representatives, approximately 5 cm length and 3 cm width. For controlled dehydration, the samples were placed in a professional oven (Genlab Drying Cabinet [17] as shown in figure 2(b)) at a controlled temperature of 40 °C. Their mass and dielectric properties were recorded by taking samples out of the oven at a regular time interval. In addition to the previous campaign data, nine liver samples were harvested to determine dehydration levels for this study. These samples were excised into small equivalent representatives and left for seven days inside the

Table 1. The biological fluid content (BC) range and the average fluid content computed considering all samples for both porcine and ovine tissues [15].

(Range of fluid content%)	
	Liver
Pigs	[68 – 72] 70%
Sheeps	[64 – 72] 70%

oven to monitor and measure their weight on days 2, 3, 4, and 7. Day 1 refers to the day of excision and when the samples were first put in the oven. The samples were allowed to dry entirely until no mass change was observed. At this point, all biological fluids and fatty matter within the sample evaporated, and the material remaining was purely dry mass. Then, the biological fluid content was calculated as the difference between the final mass and the original, representing a mass fraction of the sample. The sample database is summarized in table 1, including information about the biological fluid content (BC) range and the average fluid content computed considering all samples for each organ. The mass of the dehydrated tissues was measured using Adam Equipment (AE) [18], shown in figure 2(c).

The change in weight was monitored during the drying procedure and the respective complex permittivity was measured each day. On day 7, the liver tissue almost completely dried out and each sample was almost solid. For this reason, it was not possible to measure the dielectric properties on day 7 due to physical limitations of the open-ended coax when measuring solids.

The following sections describe in detail the fraction of the tissue's constituents and the procedure to mimic the liver using Bruggeman's model. This model was also adopted to estimate the complex permittivity at different states of dehydration. The volume fraction of the host phase was altered and the output was compared to measured dielectric data in order to choose

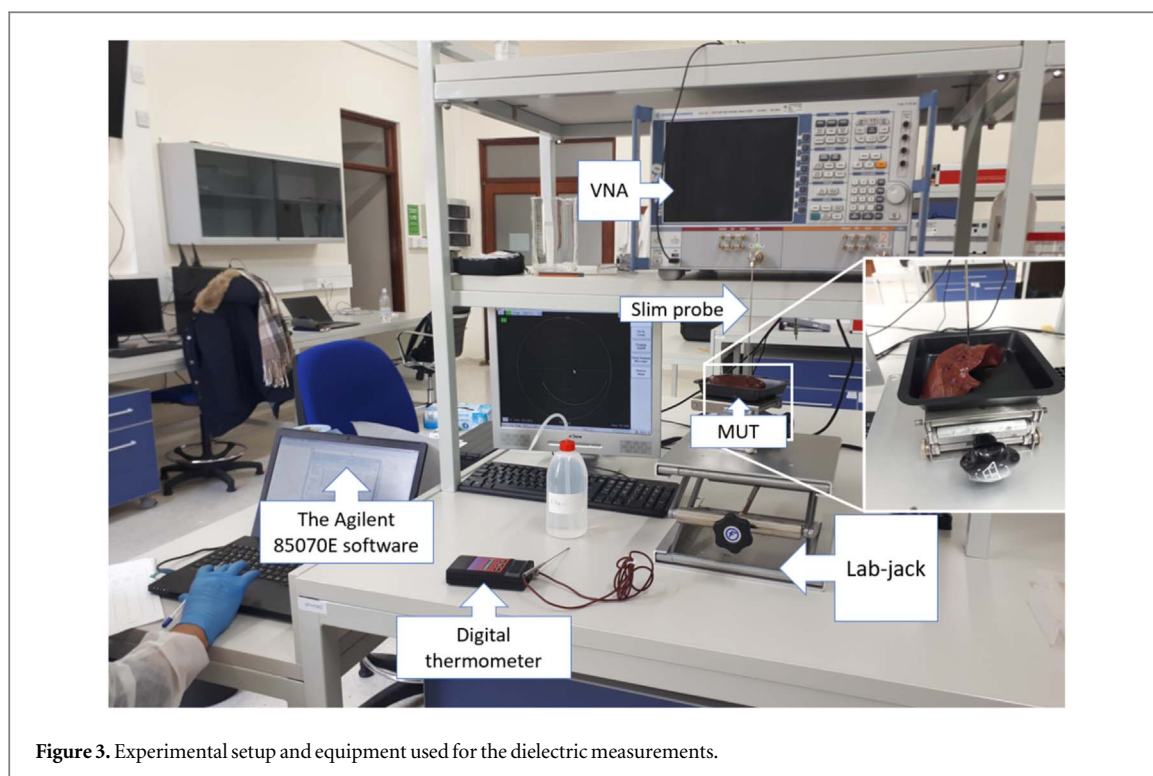


Figure 3. Experimental setup and equipment used for the dielectric measurements.

suitable concentrations for the synthesis of the mimicking solutions.

3.2. Dielectric properties measurement protocol and equipment

The measurement setup and equipment are summarized in figure 3. The experimental protocol to measure the dielectric properties prior to and during the drying process and that used for the mimicking solutions involved a selection of 3 random points. Then the mean permittivity values were calculated for each sample to ensure the obtained data's accuracy.

The Agilent Slim Form 85 070 Probe is an open-ended coaxial probe widely used to obtain the dielectric properties of a material in the form of a liquid or semisolid via its corresponding software [19] connected to a vector network analyzer (VNA). The data acquisition for the dielectric properties measurements was performed using the VNA triggered by an external computer through a GP-IB, conducting three measurements at independent locations. The VNA is a 2-port Rhode and Schwarz ZVA50 VNA, which operates in the frequency range of 10MHz to 50 GHz. The Agilent 85 070E software transforms the measured reflection coefficient via the VNA to the relevant dielectric properties. The dielectric measurements in this work contained 501 frequency points, linearly spread across the 0.5-5 GHz band. The VNA was calibrated using the software by measuring the reflection coefficient with the probe in the air; then, a shorting block was connected to the probe tip. Finally, a measurement is taken with the probe tip immersed in deionized water, whose temperature is measured using a DTM 3000 digital thermometer. In this way,

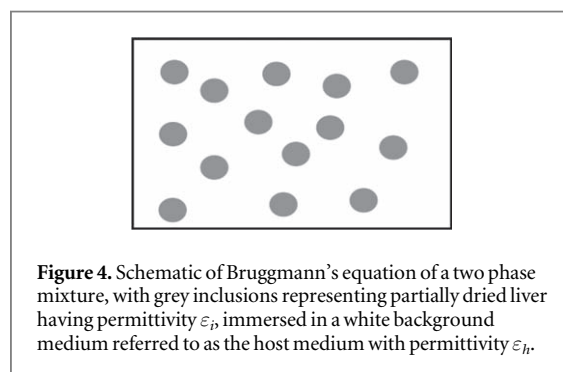
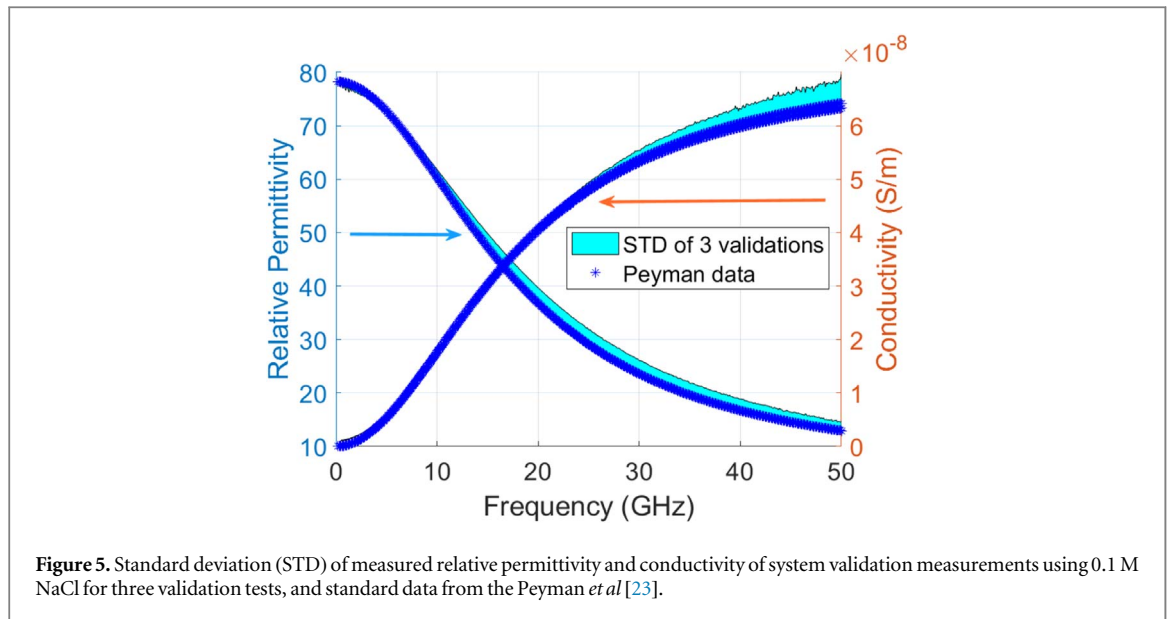


Figure 4. Schematic of Bruggmann's equation of a two phase mixture, with grey inclusions representing partially dried liver having permittivity ϵ_i , immersed in a white background medium referred to as the host medium with permittivity ϵ_h .

the VNA was fully calibrated. Before initiating the dielectric measurements, the system's calibration validation was checked by conducting a measurement on 0.1 M NaCl. The data is compared to published data in [20], the procedure is discussed in the following subsection 4.1.

3.3. Mimicking solution recipe

The tissue-mimicking simulant for liver is formed by mixtures of PBS solution as a solvent (the host medium) and the Bovine Serum Albumin (BSA) powder as the main protein content in tissues. The latter represents the solid mass fraction referred to as the inclusion phase [3]. The PBS solution was synthesized by adding two PBS tablets to 1L of deionized water. A concentration referred to as # P, for instance 12P, corresponds to 12% BSA dissolved in PBS solution. The amount of BSA to be dissolved according to the concentration desired was calculated based on dry tissue volume fraction resulting from the dry-loss procedure. From the results obtained from the



measurements discussed in section 3.1, table 1 and from a previous study conducted by Di Mio *et al.*, [15], liver contains around 70% biological fluid. Based on these results, a mimic was synthesised by using 70% PBS (40ml) solution and 30% BSA. This solution was referred to as a 30P solution. The main objective was to mimic biological fluid with a PBS solution and dry liver tissue with BSA. The motivation behind using BSA is that liver is made up mainly of hepatocytes and two of the main functions of these cells are protein synthesis and storage. Although there exist many types of different proteins, BSA is a standard chemical that is widely used in laboratories. All mixtures were stirred by means of a magnetic stirrer (using the stirrer from Witeg, Germany [21]) to ensure homogeneity of the mixture. The mimicking solutions were saved for measurement in 40ml centrifuge tubes (Isolab, Germany [22]). The measurements of the dielectric properties were taken fifteen minutes after the solutions were synthesized. Apart from the mimicking solutions, dielectric measurements at different dehydration levels were also carried out on all biological tissues at their different dehydration stages.

3.4. Numerical determination of tissue dehydration levels approach

Bruggmann mixture equation was employed to estimate the dielectric properties of liver at different dehydration levels by considering different types of host media and varying BSA concentration, see figure 4. The host agent solutions used as the solvent were 0P, 4P, 5P, 7P, 12P, PBS with 1.5 mL TX-100 and pig's blood mixed with and without heparin. The dielectric properties of these host phases were determined using the slim probe, in order to be plugged into the mixture equation. The inclusion phase used is that of the partially dried liver after leaving it three days in the oven. Ideally, completely dried liver is used as the inclusion phase, but this was not possible due to

Table 2. Measurement uncertainty of the system evaluated on 0.1 M NaCl solution.

Uncertainty	Dielectric constant (%)	Conductivity (%)
Repeatability	1.08	0.63
Accuracy	3.42	1.92
Drift	0.05	0.05
Combined	1.7	1
Percentage mean	2.67	0.07
Standard error of measurements	2.2	1.4

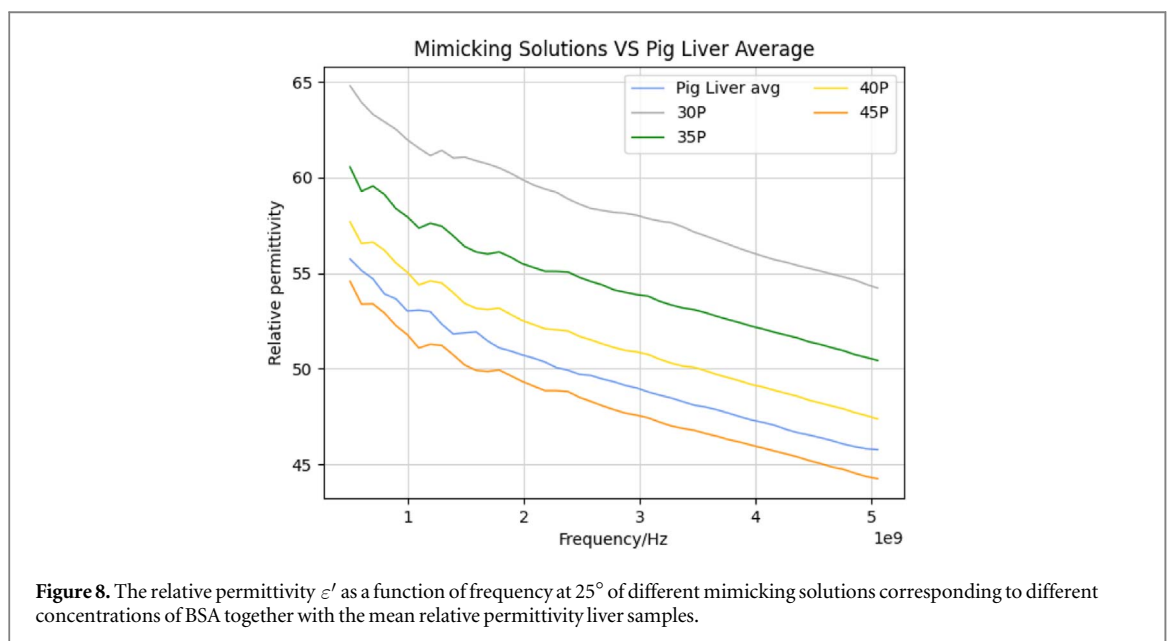
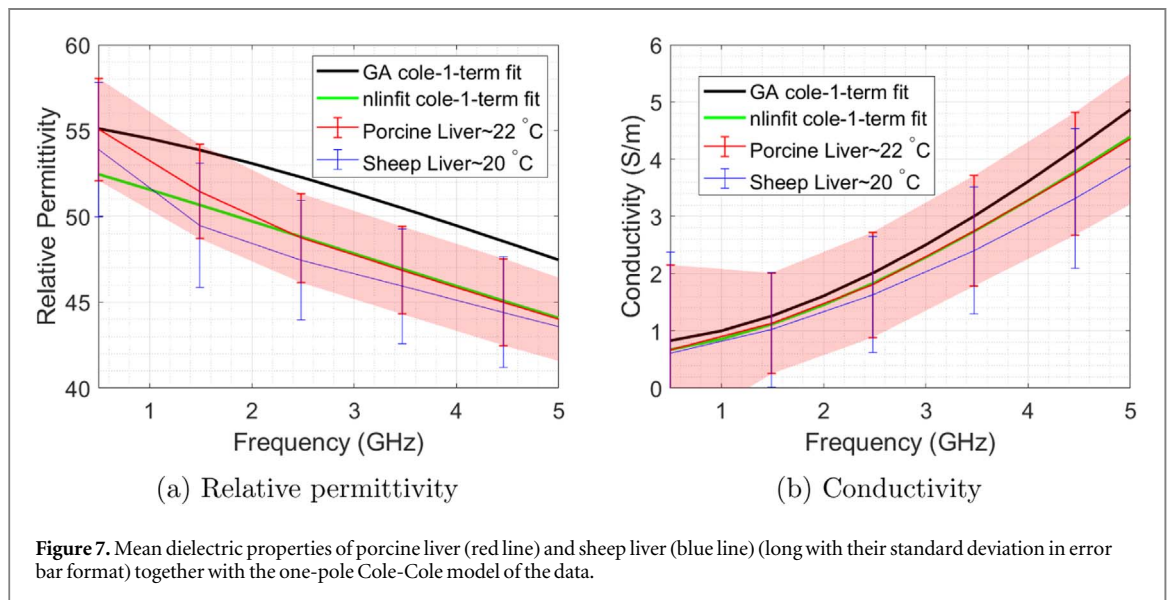
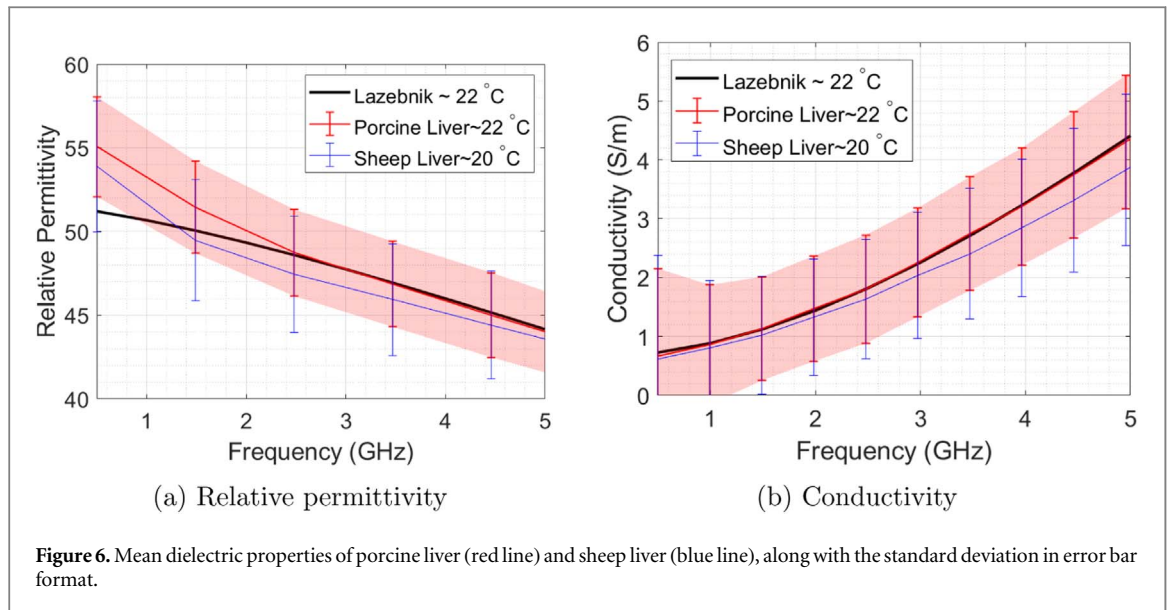
physical limitations of the open-ended probe technique when measuring irregular solids. The volume fraction was varied for each sample accordingly, i.e., in order to predict the dielectric properties of the sample on day #, the measured liver data on day # was used as the inclusion phase with the corresponding v_f of that sample on that day. However, it occurred that the 30P mixture solution overestimated the dielectric properties of the liver.

4. Results and discussion

In this section, plots of ϵ' and ϵ'' for both experimental and theoretical results are presented. Theoretical results include numerical predictions using Bruggmann two-phase mixture equation and measurements using the open-ended coax technique conducted on several tissue mimicking solutions, synthesized through dissolution of different chemicals.

4.1. Uncertainty analysis

The accuracy of the measurement system investigation employs the standard technique described in [20]. The uncertainty of the measurement system to assess



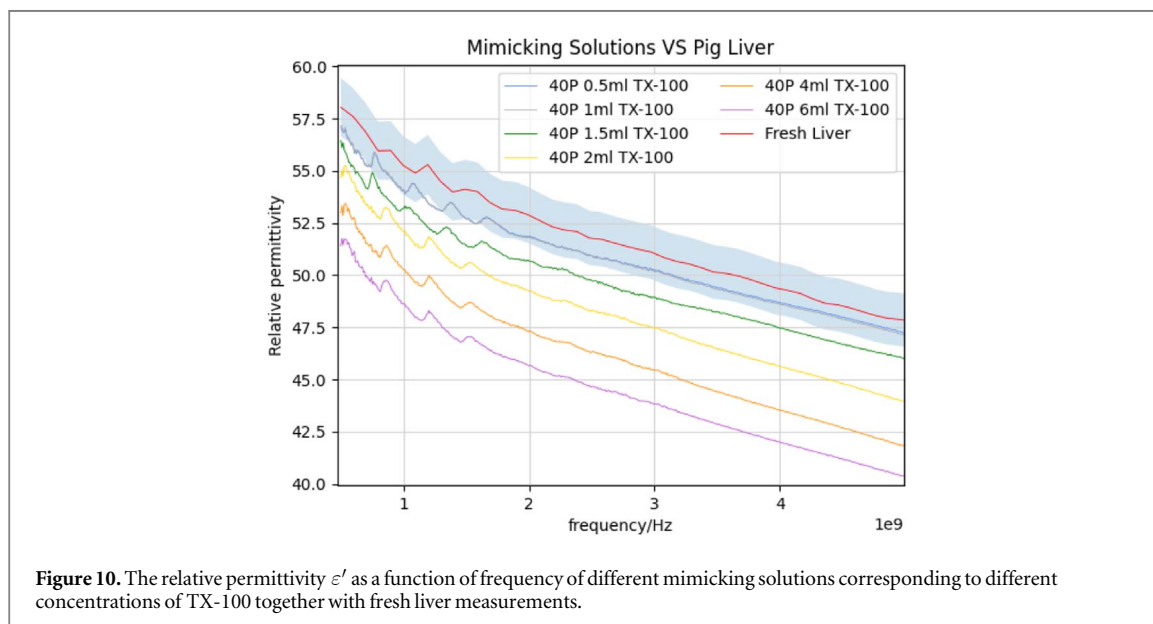
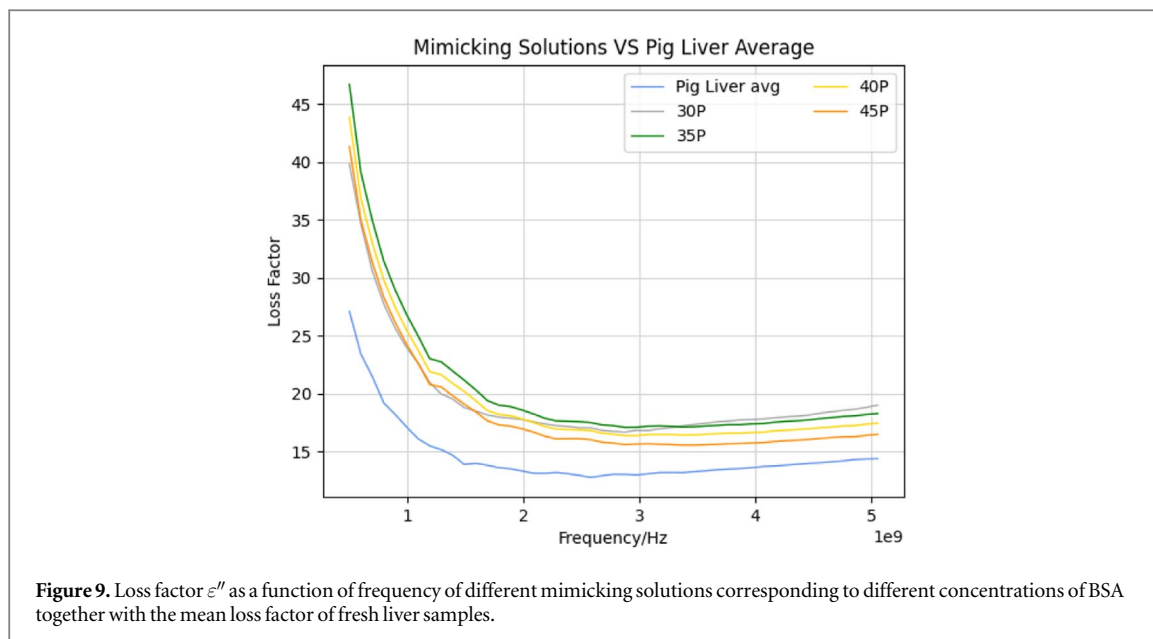
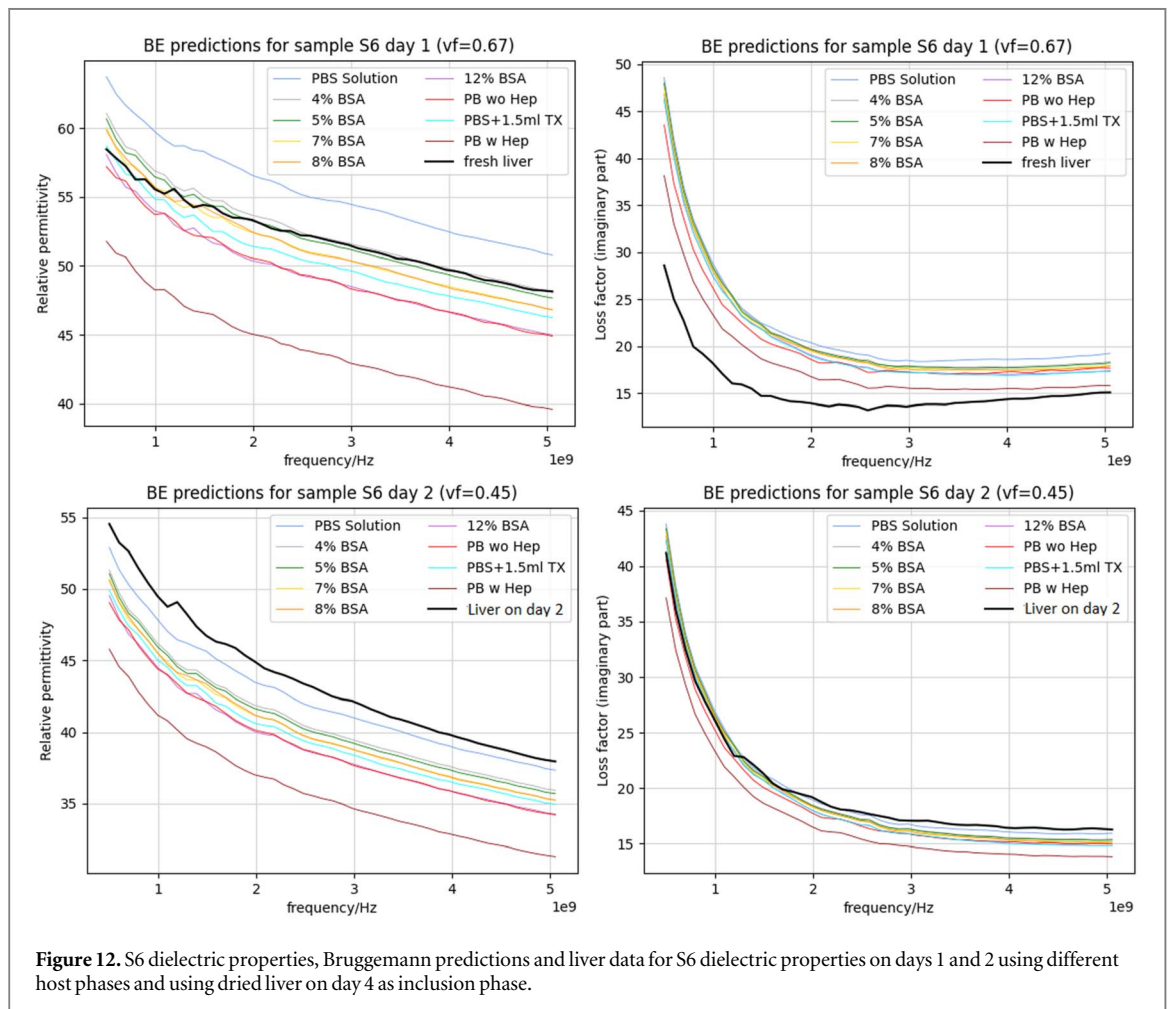
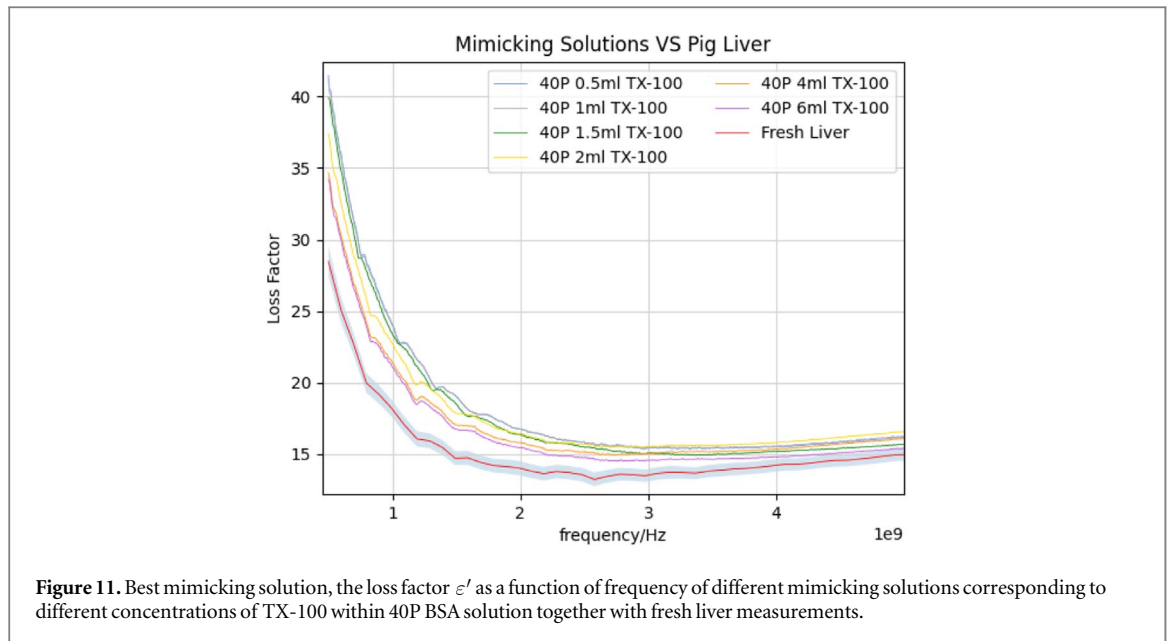


Table 3. Cole-Cole parameters of liver obtained by fitting the experimental data when measured at 25 °C.

	ϵ_s	$\pm\epsilon_s$	ϵ_{inf}	$\pm\epsilon_{inf}$	$\tau(ps)$	$\pm\tau(ps)$	$\pm\alpha$	$\pm\sigma(S/m)$	RMSE
GA fit	55.6	0.6	6.6	0.14	0.011	4.5	0.1	0.76	0.5272
non-linear fit	53.4358	0.5826	1.5008	0.1788	0.0094	1.7650	0.1847	0.5977	0.2047

random and systematic errors quantified through repeated measurements performed on 0.1 M NaCl, over a wide frequency range from 500 MHz to 50 GHz. The method implies calculating the uncertainty for each discrete frequency point and then averaging over the measurement frequency band. All the calculations were based on the deviation from the reference data of 0.1 M NaCl obtained using the Cole-

Cole model presented in Peyman *et al* [23]. Table 2 lists the random and systematic errors in the system, evaluated over 0.1 M NaCl solution at 22° C. These values confirm that the measurement system is capable of conducting dielectric measurements with high accuracy and high repeatability. Figure 5 shows a comparison between the dielectric properties of 0.1 M NaCl measured in this study, considering standard



deviation (STD) for three validation tests and the reference data acquired from the Cole-Cole model in [23]. Measured data showed good agreement with the reference data having an average error of less than 2% for the frequencies range of interest from 500 MHz to 5 GHz.

4.2. Liver dielectric properties

The relative permittivity and conductivity of liver obtained from porcine and ovine samples were measured following the measurement protocol discussed in subsection 3.2. Measurements of the complex permittivity were conducted in the frequency

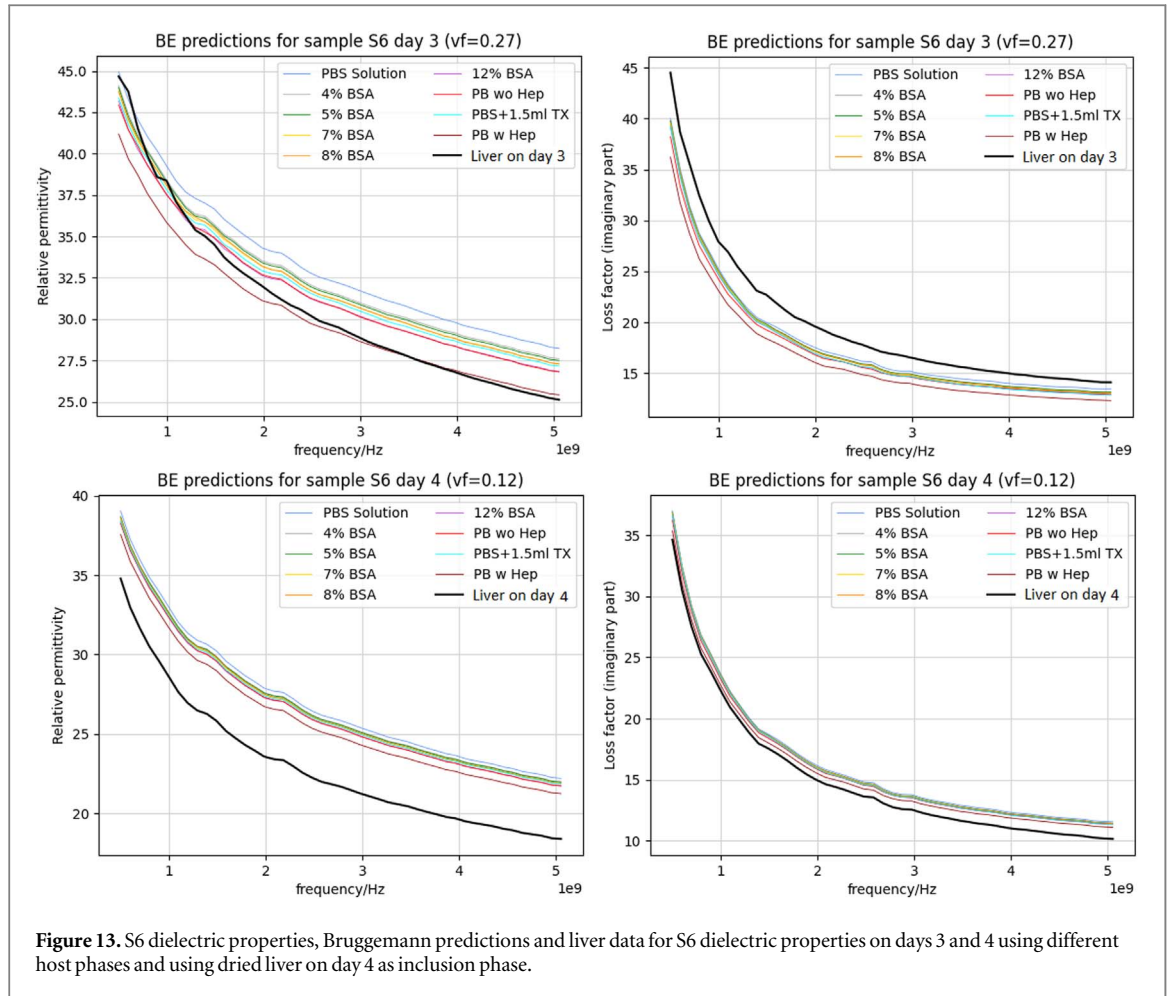


Figure 13. S6 dielectric properties, Bruggemann predictions and liver data for S6 dielectric properties on days 3 and 4 using different host phases and using dried liver on day 4 as inclusion phase.

range 500 MHz to 5 GHz and are shown in figures 6(a) and (b), respectively, along with the standard deviation.

Also, the dielectric properties of liver based on Lazebnik *et al* [24] measurements were extracted using one-pole Cole-Cole fits at 22° C spanning over frequencies 0.5–5 GHz. These are also shown in figure 6, along with the experimental results. As is evident from the plots, the liver complex permittivity trend of the sheep, porcine and of Lazebnik measurements are in good agreement and all bounded within the standard deviation range. Therefore, it may be concluded that the dielectric properties of animals are similar and can be characterised using a one-pole Cole-Cole model, given by

$$\varepsilon' - i\varepsilon'' = \varepsilon_{\infty} + \frac{\varepsilon_s - \varepsilon_{\infty}}{1 + (i\omega\tau)^{1-\alpha}} + \frac{\sigma}{i\omega\varepsilon_0} \quad (2)$$

where ε' is the relative dielectric constant, ε'' is dielectric loss factor, ω is the angular frequency, ε_s is the static dielectric constant, τ is the relaxation time, α is the broadening parameter of the realization, and ε_{inf} is the permittivity at high frequency.

Figures 7(a) and (b) show the dielectric properties of liver against frequency along with the one-pole Cole-Cole fits to the experimental data. In this work, the parameters are fitted first with a genetic algorithm optimisation (GA), the details of the technique is

described in [25], as starting estimates and then tuned with a non-linear least square regression. The fitted parameters to the Cole-Cole model and the 95% confidence intervals associated with each parameter are shown in table 3. Included in this table are the root mean square error (RMSE) values of each fit.

4.3. Mimicking solutions

The synthesis of 35P, 40P and 45P were set for liver verification. As observed from figures 8 and 9, the 40P and 45P solutions appear to be the best mimics. However, dielectric properties are still being over-estimated by the 40P solution and underestimated by the 45P solution. Therefore, in order to better simulate the dielectric properties of the liver, a different component was considered by adding different concentrations, 0.5 ml, 1 ml, 1.5 ml, 2 ml, 4 ml, and 6 ml, of Triton X-100 (TX-100 which is a surfactant) to the 40P solution. Since it is a surfactant, it is expected to lower the relative permittivity, and therefore it was added to the 40P solution rather than to the 45P solution. It turned out that around 1 ml TX-100 in conjunction with 40P solution produces the best agreement for relative permittivity, as can be seen in figure 10. However, the loss factor was best mimicked by a concentration of 6ml TX-100 inside the 40P solution, as can be seen in figure 11. The result

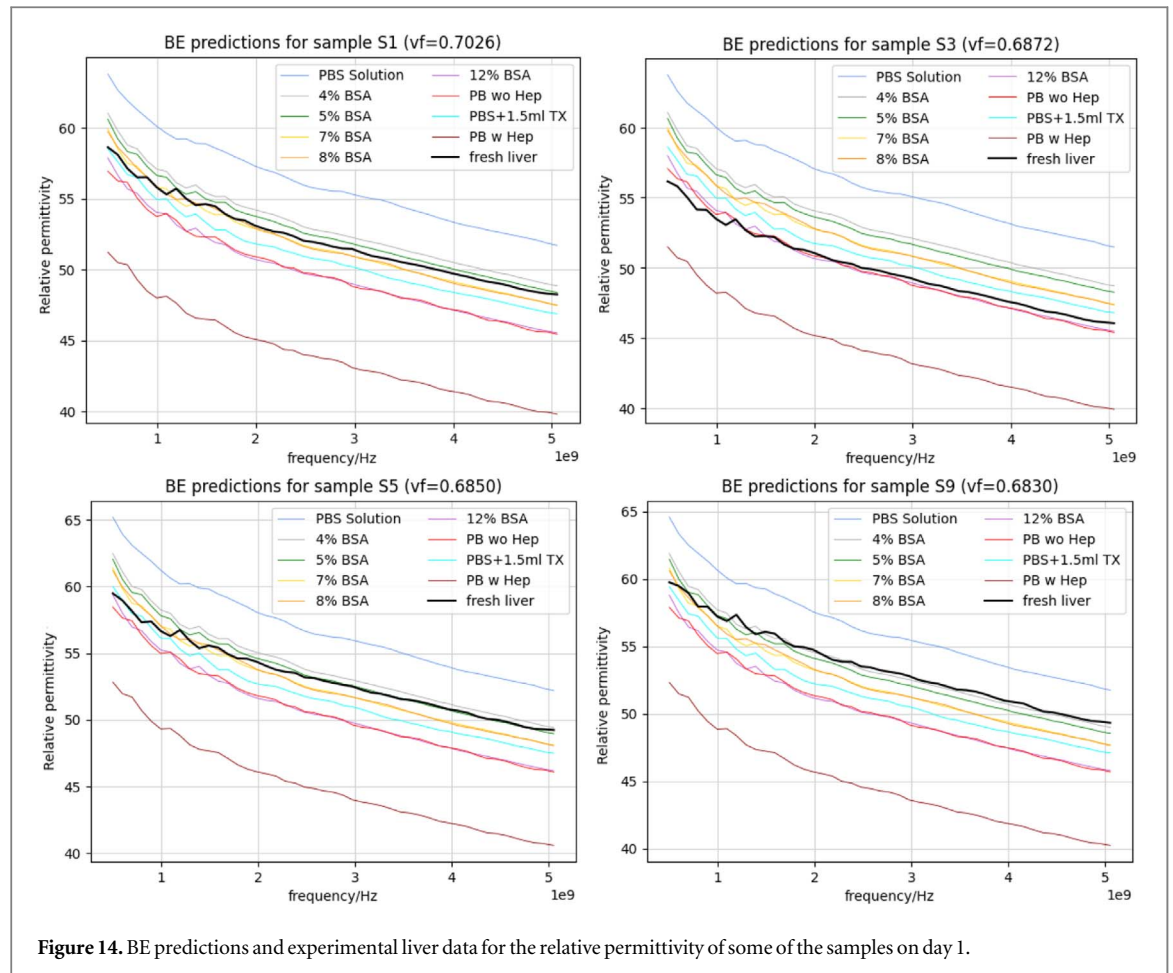


Figure 14. BE predictions and experimental liver data for the relative permittivity of some of the samples on day 1.

Table 4. A summary of percentage of fluid lost per day and per sample.

	Day 1 (Fresh)	Day 2		Day 3		Day 4		Day 7	
	Mass / g	Mass / g	% loss	Mass / g	% loss	Mass / g	% loss	Mass / g	% loss
s1	31.295	20.368	34.9	14.845	52.6	11.63	62.8	9.308	70.3
s2	59.372	42.745	28	32.114	45.9	25.219	57.5	18.946	68.1
s3	29.413	20.443	30.5	14.466	50.8	11.362	61.4	9.199	68.7
s4	34.717	24.941	28.2	19.394	44.1	15.739	54.7	11.229	67.7
s5	45.614	32.875	27.9	24.283	46.8	19.089	58.2	14.367	68.5
s6	69.403	53.976	22.2	41.154	40.7	31.391	54.8	22.565	67.5
s7	34.638	23.458	32.3	16.723	51.7	13.108	62.2	10.281	70.3
s8	36.522	23.963	34.4	17.777	51.3	13.786	62.3	10.877	70.2
s9	60.978	44.332	27.3	33.282	45.4	26.375	56.8	19.331	68.3

obtained for the loss factor lies outside the associated uncertainty range, and is therefore less reliable and relevant than the result obtained for the relative permittivity. When considering both figures (10 and 11) it seems that around 1.5ml TX-100 inside a 40P solution provides the best mimicking solution.

The Bruggeman equation was employed to verify the inclusion phase and the host medium volume fractions. It was found that substituting a percentage of 0.7 as fluid volume fraction (ϵ_e), represented by the dielectric properties of PBS solution with 1.5ml TX-100 as host phase, and dehydrated liver (liver on day 4) as

inclusion phase (ϵ_i), represents the best simulation of fresh liver permittivity.

The main limitation of the open-ended coax probe spectroscopy for the determination of dielectric permittivity that it has to penetrate into the tissue and no air gaps should be present throughout the sensing volume around the probe tip. For this reason, the complex permittivity of solids cannot be measured accurately using the open-ended probe technique. Hence, the disadvantage is the inability to use it on samples from day 7 and onward of the thermogravimetric procedure as the samples undergo degradation

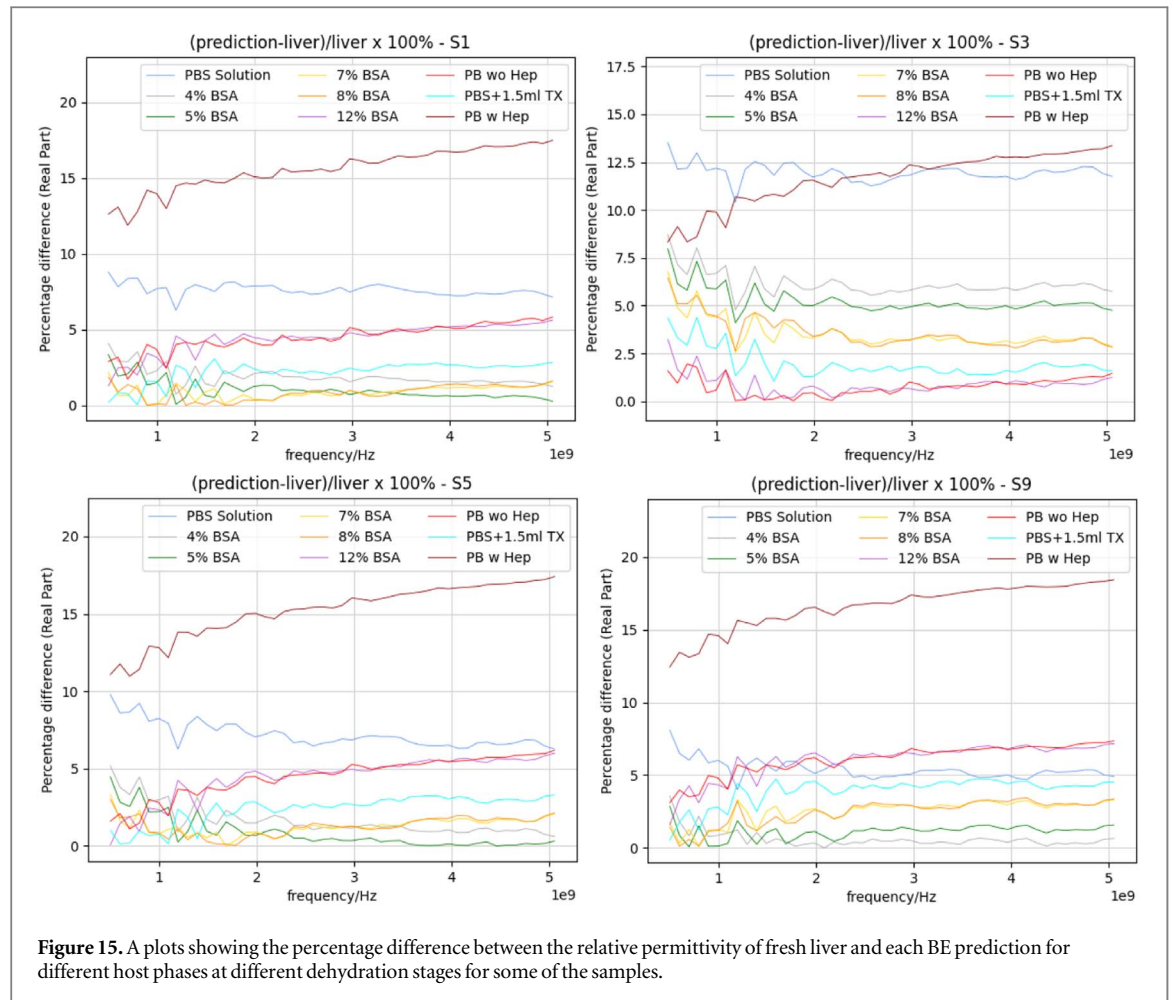


Figure 15. A plots showing the percentage difference between the relative permittivity of fresh liver and each BE prediction for different host phases at different dehydration stages for some of the samples.

of their moisture content and their surface become robust.

4.4. Bruggemann's equation to mimic different dehydration levels

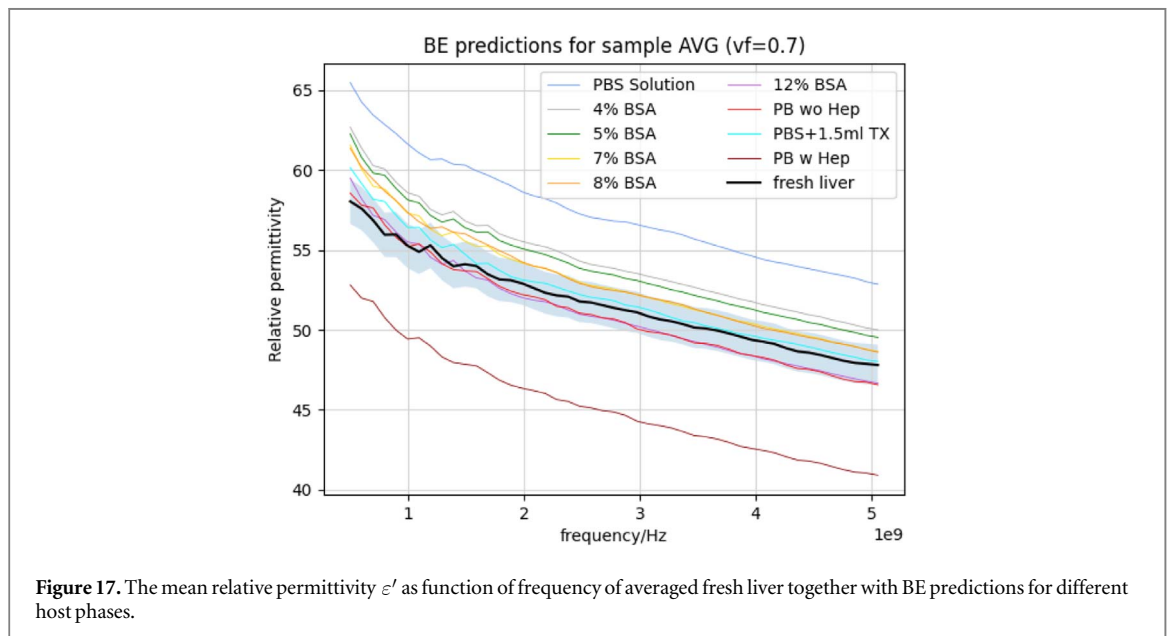
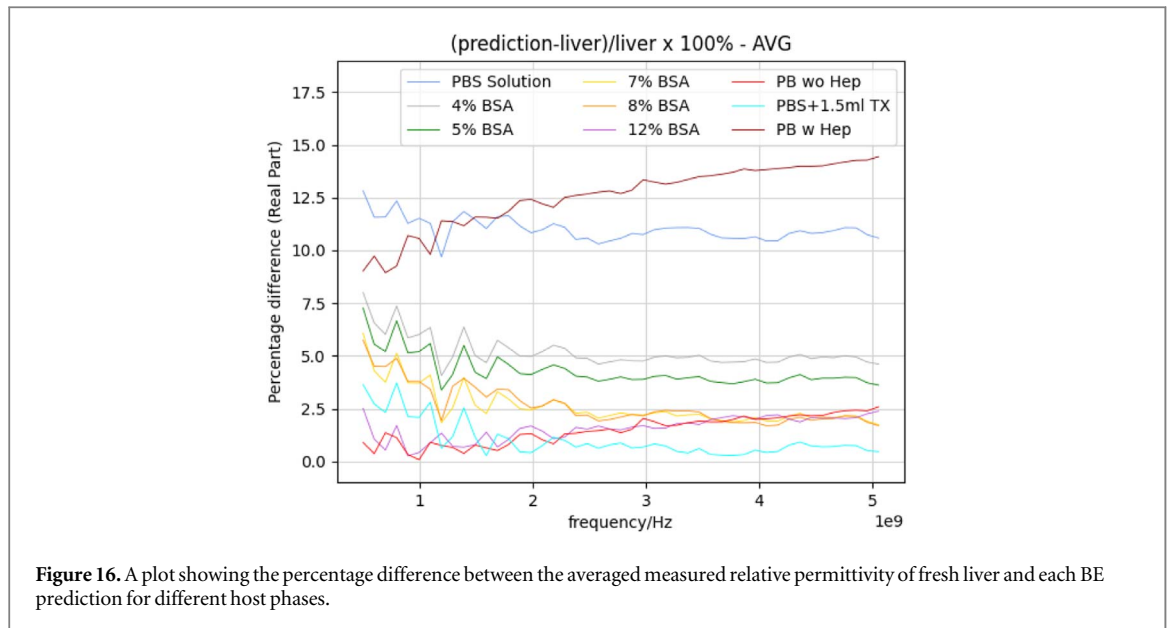
In this section the Bruggemann equation (BE) is used to model the dielectric properties of liver at different dehydration levels. Different host media, mainly 0P, 4P, 5P, 7P, 8P, 12P, porcine blood with and without heparin and PBS solution with 1.5 ml TX were considered, whilst keeping the inclusion phase as the dielectric properties of dry liver as at day 4 (see table 4). In order to calculate the hydration levels of each sample, the mass of the dehydrated sample on each day, was subtracted from the mass of the fresh sample on day 1. The change in mass corresponded to the biological fluid lost by the sample till that day, as shown in table 4. The percentage of mass lost on each day was then used as the volume fraction within the BE to simulate the dielectric properties of liver at different dehydration stages (see table 4).

The BE prediction results were then compared with liver dielectric properties of the same drying stage. The findings for S6 (which happened to be the largest ample) are shown in figures 12 and 13. Furthermore, The results when varying the different host

phases are presented graphically for the relative permittivity of fresh samples S1, S3, S5 and S9 in figure 14. The volume fraction for the host phase used for fresh liver corresponds to the percentage of biological fluid lost by completely dried liver (day 7), even though dielectric data from day 4 is used for the inclusion phase.

It can be seen from these figures that for day 1 the BE prediction of the relative permittivity demonstrates a reasonable agreement with different host media, 4P, 8P and PBS solution with 1.5 ml TX. However, this agreement degrades gradually at different dehydration stages throughout the drying process from day 1, day 2, day 3, and day 4. On the other hand, BE prediction of the loss factor of the dehydrated liver exhibits inconsistent behaviour. There is significant disagreement with the values of the fresh liver loss factor on day 1 and at each dehydration stage the trend of the imaginary values of the dielectric properties converge to a reasonable agreement on day 4. The figures clearly illustrate that even though none of the hosts provide an adequate mimic, porcine blood with heparin is the best candidate to simulate the loss factor of liver.

The percentage difference between the relative permittivity of fresh liver and each BE prediction of different host phases was calculated to determine the



best host solution mimic. The adopted procedure compares the percentage difference between BE-predicted and measured values for each liver sample relative to volume fraction ν_f as shown in figure 15. The percentage difference between the average relative permittivity of all samples and the BE predictions with average ν_f was evaluated figure 16.

It can be concluded from figures 15 and 16 that at frequencies lower than 2GHz, porcine blood without heparin and the 12% BSA solutions constitute the best host. However, at frequencies higher than 2 GHz, the 40ml PBS + 1.5ml TX-100 solution is the optimal host. From a plot of the average relative permittivity of liver and BE simulations (Figure 17), it is shown that on average a PBS solution + 1.5ml TX-100 is indeed the optimal host phase. The fact that the BE simulations are very similar to the experimental data obtained is very

promising and supports results obtained from a previous study conducted on muscle tissue [3].

5. Conclusion

This paper presents a correlation between a numerical mixture model and an experimental implementation of the two-phase liver simulant. The fact that the Bruggeman two-phase mixture equation produced similar results to what was found experimentally supports its application in modelling the relative permittivity of the liver and at different states of dehydration for samples undergoing 10%–20% weight loss whilst drying.

The dielectric properties of porcine liver samples were measured in the frequency range from 0.5 to

5 GHz. For each sample, three independent measurements were conducted. The volume fractions corresponding to the percentage physiological fluid content in the liver were obtained using the loss-on-drying method and were substituted into the mixture model. The experimental result show that the 40P + 1.5 ml TX-100 solution is a good simulant for the relative permittivity of fresh porcine liver tissue.

One of the main advantages of such liquid solutions is that they are relatively easy to produce and can be prepared within a few minutes, given that the necessary apparatus and chemicals are made available. There also exists the possibility of using the liquid solution as a culture medium for growing cancerous cells inside it. Certain medical applications such as microwave imaging can then be tested using the solution itself. This makes the development and research of dielectric spectroscopy mimicking solutions an active and growing field of study which has gained much traction and interest over the last decade.

Data availability statement

All data that support the findings of this study are included within the article (and any supplementary files).

ORCID iDs

Iman Farhat  <https://orcid.org/0000-0001-8401-997X>
Jonathan Farrugia  <https://orcid.org/0000-0003-1782-3903>
Lourdes Farrugia  <https://orcid.org/0000-0002-1816-0657>
Julian Bonello  <https://orcid.org/0000-0002-1816-0657>
Daphne Pollacco  <https://orcid.org/0000-0003-3723-6626>
Charles Sammut  <https://orcid.org/0000-0002-8138-3052>

References

- [1] Lazebnik M, Madsen E L, Frank G R and Hagness S C 2005 Tissue-mimicking phantom materials for narrowband and ultrawideband microwave applications *Phys Med Biol.* **50** 4245–58
- [2] Fang Q, Meaney P M and Paulsen K D 2004 Microwave image reconstruction of tissue property dispersion characteristics utilizing multiple-frequency information *IEEE Trans. Microwave Theory Tech.* **52** 1866–75
- [3] Pollacco D A, Farrugia L, Conti M C, Farina L, Wismayer P S and Sammut C V 2019 Characterization of the dielectric properties of biological tissues using mixture equations and correlations to different states of hydration *Biomedical Physics and Engineering Express* **5** 035022
- [4] McGarry C K et al 2020 Tissue mimicking materials for imaging and therapy phantoms: a review *Physics in Medicine & Biology* **65** 23TR01
- [5] Sieryi O, Popov A, Kalchenko V, Bykov A and Meglinski I 2020 Tissue-mimicking phantoms for biomedical applications *SPIE Photonics Europe* 11363 ed V V Tuchin, W C P M Blondel and Z Zalevsky pp 111–7
- [6] Phantom Imaging. Available from: https://en.wikipedia.org/wiki/Imaging_phantom.
- [7] Amiri S A, Berckel P V, Lai M, Dankelman J and Hendriks B H W 2022 Tissue-mimicking phantom materials with tunable optical properties suitable for assessment of diffuse reflectance spectroscopy during electrosurgery *Biomed. Opt Express.* **13** 2616–43
- [8] Forte A E, Galvan S, Manieri F, Rodriguez y Baena F and Dini D 2016 A composite hydrogel for brain tissue phantoms *Materials & Design.* **112** 227–38
- [9] Lan S W et al 2016 Preparation of a carbon doped tissue-mimicking material with high dielectric properties for microwave imaging application *Materials* **9** 559 (<https://www.mdpi.com/1996-1944/9/7/559>)
- [10] Ahmad M S et al 2020 Chemical characteristics, motivation and strategies in choice of materials used as liver phantom: a literature review *Journal of Medical Ultrasound* **28** 7–16
- [11] Andreuccetti D, Bini M, Ignesti A, Olmi R, Rubino N and Vanni R 1988 Use of polyacrylamide as a tissue-equivalent material in the microwave range *IEEE Trans. Biomed. Eng.* **35** 275–7
- [12] Stauffer P R, Rossetto F, Prakash M, Neuman D G and Lee T 2003 Phantom and animal tissues for modelling the electrical properties of human liver *Int. J. Hyperth.* **19** 89–101
- [13] Cortese L et al 2018 Liquid phantoms for near-infrared and diffuse correlation spectroscopies with tunable optical and dynamic properties *Biomedical Optics Express.* **9** 2068
- [14] Bruggeman A G D 1935 Berechnung verschiedener physikalischer Konstanten von heterogenen Substanzen. I. Dielektrizitätskonstanten und Leitfähigkeiten der Mischkörper aus isotropen Substanzen *Annalen der Physik.* **416** 636–64
- [15] Meo S D et al 2021 The variability of dielectric permittivity of biological tissues with water content *J. Electromagn. Waves Appl.* **36** 48–68
- [16] Youngs I J, Treen A S, Fixter G and Holden S 2002 Design of solid broadband human tissue simulant materials. Science, Measurement and Technology *IEE Proceedings* **149** 323–8
- [17] Warming Cabinets: (<https://www.genlab.co.uk/65-drying-warming-cabinets>)
- [18] AE: <https://www.adamequipment.com/products/precision-balances>
- [19] Keysight N1501A Dielectric Probe Kit 10 MHz to 50 GHz. Available from: <https://www.keysight.com/zz/en/assets/7018-04631/technical-overviews/5992-0264.pdf>
- [20] Gabriel C and Peyman A 2006 Dielectric measurement: error analysis and assessment of uncertainty *Physics and Medical Biology* **51** 6033–46
- [21] WITEG; Available from: <https://www.witeg.de/en/products/laboratory-equipment/heating/magnetic-stirrer-with-hotplate/magnetic-stirrer-with-hotplate-msh-a-analog-700c-to-3800c-up-to-1500rpm>
- [22] ISOLAB; Available from: <https://www.isolab.de/en-us/life-science-microscopy-microbiology/tubes-centrifuge-clear-conicalbottom-screwcap>
- [23] Peyman A, Gabriel C and Grant E H 2007 Complex permittivity of sodium chloride solutions at microwave frequencies *Bioelectromagnetics* **28** 264
- [24] Lazebnik M, Converse M C, Booske J H and Hagness S C 2006 Ultrawideband temperature-dependent dielectric properties of animal liver tissue in the microwave frequency range *Phys. Med. Biol.* **51** 1941–55
- [25] Clegg J and Robinson M P 2010 A genetic algorithm used to fit the Debye functions to the dielectric properties of tissues *IEEE Congress on Evolutionary Computation* **1** 1–8